Characterization and Application of Nanomaterials (2019) Volume 2 Issue 2
doi:10.24294/can.v2i2.813

REVIEW ARTICLE

Interaction of light with lead halide perovskites: A review

Zhiya Dang*, Duc Anh Dinh

Nanochemistry Department, Istituto Italiano di Tecnologia, via Morego 30, 16163 Genova, Italy. E-mail: rongmeijiao yin@gmail.com

ABSTRACT

Lead halide perovskites are the new rising generation of semiconductor materials due to their unique optical and electrical properties. The investigation of the interaction of halide perovskites and light is a key issue not only for understanding their photophysics but also for practical applications. Hence, tremendous efforts have been devoted to this topic and brunch into two: (i) decomposition of the halide perovskites thin films under light illumination; and (ii) influence of light soaking on their photoluminescence (PL) properties. In this review, we for the first time thoroughly compare the illumination conditions and the sample environment to correlate the PL changes and decomposition of perovskite under light illumination. In the case of vacuum and dry nitrogen, PL of the halide perovskite ($MAPbI_{3-x}Cl_x$, $MAPbBr_{3-x}Cl_x$, $MAPbI_3$) thin films decreases due to the defects induced by light illumination, and under high excitations, the thin film even decomposes. In the presence of oxygen or moisture, light induces the PL enhancement of halide perovskite ($MAPbI_3$) thin films at low light illumination, while increasing the excitation, which causes the PL to quench and perovskite thin film to decompose. In the case of mixed halide perovskite ($(MA)Pb(Br_xI_{1-x})_3$) light induces reversible segregation of Br domains and I domains.

Keywords: Lead Halide Perovskites; Light Illumination; Photoluminescence; Decomposition; Segregation

ARTICLE INFO

Article history:
Received 9 October 2019
Received in revised form 2 November 2019
Accepted 5 November 2019
Available online 19 November 2019

1. Introduction

Lead halide perovskites (LHPs), with the chemical formula of $APbX_3$ (A = Cs, CH_3NH_3 (MA), $CH(NH_2)_2$ (FA), X = Cl, Br, I), have emerged as the new generation of intriguing semiconductor materials for solar cells[1-4], lasers[5,6], light emitting diodes[3,5], and photodetectors[7,8] in recent years. The rapid development of LHPs in these fields arises from the ease of processability, as well as their unique optical and electrical properties, such as small exciton binding energy, long exciton diffusion lengths, low charge recombination, high absorption coefficient, a direct bandgap and its tunability over near-infrared, visible to ultraviolet range[9-15]. One of the major obstacles hindering the industrialization of LHPs is the toxicity of lead (Pb), for which lead-free halide perovskites have been widely explored to replace Pb with non-toxic metals, such as Mn(II), Sn(II), Sn(IV), Bi(III), Sb(III), Cu(II) etc.[16-22]. Another important issue is the instability of LHPs upon exposure to the polar solvents and ambient atmospheric conditions (heat, moisture, oxygen), or radiations, such as electron and X-ray beams, originating from the low energy barrier for the halide perovskite crystal formation, and till now this still remain as a critical issue in various applications[23-30]. The LHPs degrade via different paths under the above mentioned conditions. In the presence of moisture, the degradation path of $MAPbI_3$ films as well as single crystals is initiated by for-

mation of hydrated intermediates, e.g., both monohydrate $CH_3NH_3PbI_3 \cdot H_2O$ and dihydrate $(CH_3NH_3)_4PbI_6 \cdot 2H_2O$, and the reaction can be described by the reversible chemical equations of:

$4CH_3NH_3PbI_3 + 4H_2O \leftrightarrow 4[CH_3PbI_3 \bullet H_2O] \leftrightarrow (CH_3NH_3)_4PbI_6 \bullet 2H_2O + 3PbI_2 + 2H_2O$[24,31,32]

The $MAPbCl_3$, $MAPbBr_3$ and $MAPbI_3$ are found to decompose into PbX_2, gaseous methylamine CH_3NH_2 and HX, when they are heated under low-temperature (25-150°C)[33,34]. In the case of low energy electron beam irradiation of $MAPbI_3$ thin film (4.5 to 60 eV), the material degrades with the reaction described by:

$CH_3NH_3PbI_3 \xrightarrow{e^- \rightarrow C-N\ breakage} (-CH_2-) + NH_3 + HI + PbI_2$[35]

While for $CsPbX_3$ nanocrystals in a TEM (80/200KeV), through a radiolysis process, Pb^{2+} ions are reduced to metallic Pb atoms along with the oxidation and desorption of halogen species in the vacuum. The Pb atoms further aggregate to form Pb nanoparticles at higher temperatures (above-40°C) while below -40°C the perovskites decompose into CsX, PbX_2 and CsPb domains and further halogen desorption eventually leads to only Cs and Pb species[27,28,36]. Under other types of radiations such as X-ray, halogen loss and reduction of Pb are also found to occur[27,29].

Not only unstable in moisture, oxygen, heat or radiation conditions, the LHPs are also sensitive under light[26,37,38]. Doomed to interplay with light, the investigation of interaction of halide perovskites and light is a key issue for understanding their photophysics and for characterization and practical applications, because the optical characterization techniques such as photoluminescence and absorption measurements as well as working of perovskite based devices such as solar cell, LEDs, lasers, and photodetectors, involve the interaction of halide perovskites with light. The LHPs are fabricated and applied in several forms, e.g., polycrystalline thin film with micron-size domains (mainly for organic-inorganic type $MAPbX_3$), single crystals (also for MA-PbX_3), and nanocrystals (available for all cation types $CsPbX_3$, $MAPbX_3$, $FAPbX_3$). A large amount of literatures report the decomposition of $MAPbX_3$ perovskite thin films and single crystals upon light illumination[39-41]. On the other hand, light is found to cause enhancement and quenching of photoluminescence (PL) of $MAPbX_3$ perovskite film[42-44]. Moreover, an unusual light-induced effect, photo-induced halide segregation is also reported in $(MA)Pb(Br_xI_{1-x})_3$ thin films[45-51]. In the present review, we summarize the above aspects and attempt to discuss some of the seemingly conflicting views on the interaction of perovskite and light.

2. Light illumination on halide perovskite thin films

2.1 Oxygen-free and moisture-free environment

The literatures on the light illumination effect of halide perovskite thin films in dry N_2 or vacuum are summarized in **Table 1**.

Table 1. The literatures of light illumination on halide perovskite in vacuum or dry N_2

Material	Light illumination	Environment	Film morphology	PL	Ref
$MAPbI_3$ film	405 nm laser, 0.5 W/cm^2 for 5 mins (dose: 150 J/ cm^2)	Nitrogen, vacuum	Not reported	PL decreases	[52]
$MAPbI_{3-x}Cl_x$, $MAPbBr_{3-x}Cl_x$ film	White light source, 0.0434 W/cm^2, for 24 h(89994 J/ cm^2)	Nitrogen	Almost stable	Not reported	[41]
$MAPbI_3$ film	408 nm, 0.68 W/cm^2 for 2 hours (dose: 4896 J/ cm^2)	Vacuum	Decomposition	Not reported	[40]
$MAPbI_{3-x}Cl_x$, $MAPbBr_{3-x}Cl_x$ film	White light source, 0.0434 W/cm^2, for 2 h (7499 J/ cm^2)	Vacuum	Decomposition	PL decreases	[41]
$MAPbI_3$ film	532 nm laser, 140 to 4000 W/cm^2 for Seconds (dose: 1000 to 20000 J/ cm^2)	Vacuum	Decomposition	PL decreases	[38]
$MAPbI_3$ film	470 nm laser, 0.2 to 0.9 W/cm^2 for 7 mins (84 to 378 J/ cm^2)	Encapsulated		Continuous enhancement	[44]
$MAPbI_3$ film	470 nm laser, 1.6 to 4.6 W/cm^2 for few mins (1200 J/ cm^2)	Encapsulated	may involve decomposition	Continuous quenching	[44]

Both the excitation power (W/cm^2) and dose (J/cm^2) of light matters, and an absolute comparison of these parameters cannot be made due to discrepancies in the wavelength, type of source (continu-

ous or pulsed), and fabrication method of samples. However, a rough comparison can give useful guidance on better understanding how light and perovskite interact. In nitrogen, PL of perovskite films drops over time under illumination (at power of 0.04 to 0.5W/cm^2, dose of 150 to 89994 J/cm^2) because illumination induces the defects in the $MAPbX_3$ films, yet the films are found to hardly degrade[41,52]. In vacuum, PL drops even more, and according to literatures at certain illumination conditions such as power of 0.04 to 4000 W/cm^2, dose above 1000 J/cm^2 the material is found to decompose through the following equations (1, 2)[38,40]:

$$CH_3NH_3PbI_3 \xrightarrow{light} (\text{-}CH_2\text{-}) + NH_3 + HI + PbI_2 \quad (1)$$

$$PbI_2 \xrightarrow{light} Pb + I_2 \quad (2)$$

As the above equations show the decomposition products include volatile NH_3, HI, and I_2. In nitrogen environment, the desorption of gaseous products is suppressed and therefore no obvious decomposition of the film is observed. However, in vacuum, these products are immediately desorbed which promotes the decomposition process, and the unreacted $CH_3NH_3PbI_3$, metallic Pb, and carbon hydrocarbonaceous species remain on the surface, as demonstrated by the upper row of schematics in **Figure 1A**[40]. There is a saturation of decomposition, which is about 33%, as is schematically shown by lower row of **Figure 1A**, and indicated by the change of Pb^{2+} signal and Pb^0 signal in XPS spectra at different durations of illumination in **Figure 1B**[40].

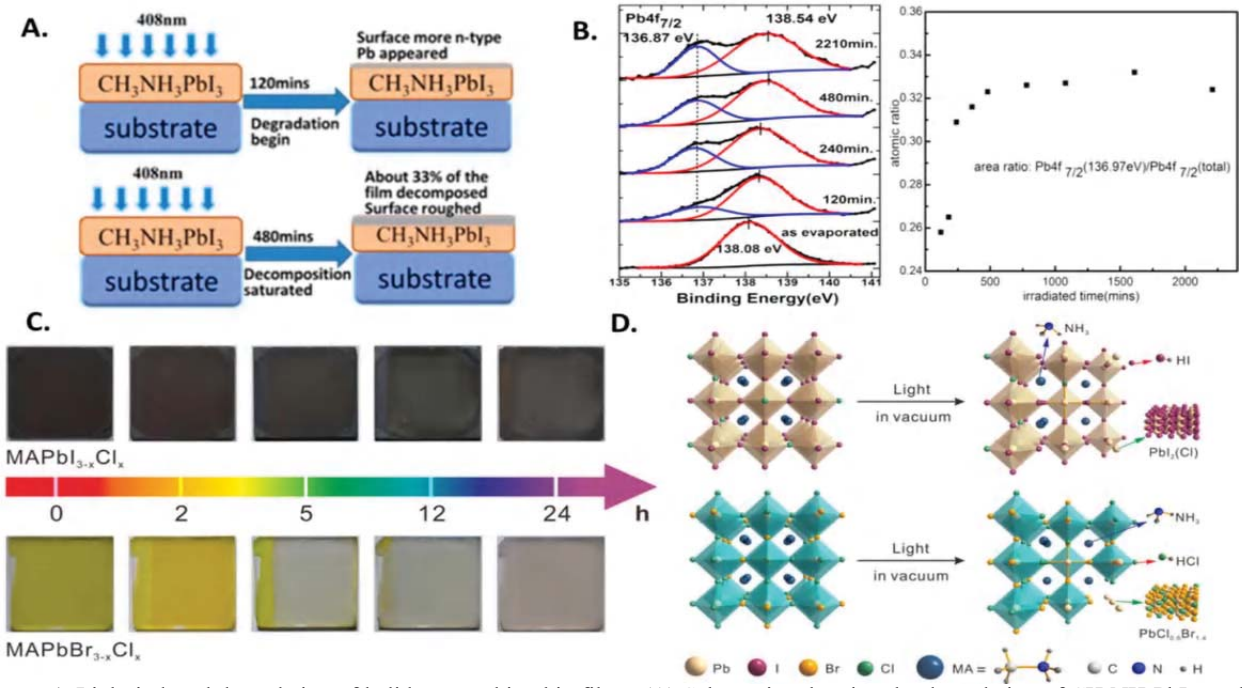

Figure 1. Light induced degradation of halide perovskite thin films: **(A)** Schematics showing the degradation of $CH_3NH_3PbI_3$, under light illumination; **(B)** XPS data on Pb 4f7/2 and metallic Pb fraction during light illumination showing the saturation of degradation; **(C)** Optical images of $MAPbI_{3-x}Cl_x$ and $MAPbBr_{3-x}Cl_x$ perovskites films with various illumination durations; **(D)** Schematics of the light-induced degradation processes for perovskite films of $MAPbI_{3-x}Cl_x$ and $MAPbBr_{3-x}Cl_x$. **(A, B)** reproduced with permission from Li *et al.*[40], Copyright (2017) American Chemical Society; **(C, D)** reproduced with permission from Xu[41], Copyright (2018) American Chemical Society**.**

A similar degradation also occurs for perovskite thin film with mixed halide of iodine and clorine, as well as bromine and clorine under light illumination, which was studied by Ruipeng Xu *et al* in detail: $CH_3NH_3PbI_{3-x}Cl_x$ and $CH_3NH_3PbBr_{3-x}Cl_x$ films are found to undergo degradation process as is shown by the optical images in **Figure 1C**[41]. In this degradation process, the illumination breaks the chemical bonds between CH_3NH_3 and Pb, besides, the C–N bonds in CH_3NH_3 and the CH_3NH_3 cation convert from the crystal form to hydrocarbon species, demonstrated by the schematics in **Figure 1D**[41]. Further light illumination causes different behaviour in these two mixed halide perovskite materials: in the case of $CH_3NH_3PbI_{3-x}Cl_x$, light illumination further breaks the Pb–I bonds in PbI_2 and induces the conversion of Pb^{2+}in PbI_2 into metallic Pb, and iodine sublimes into gaseous form, while such results are not observed in the case of $CH_3NH_3PbBr_{3x}–Cl_x$[41]. The above mentioned processes

can be summarized by the following chemical equations (3, 4, 5):

$$CH_3NH_3PbI_{3-x}Cl_x \xrightarrow{light} (-CH_2-) + NH_3 + HI + PbI_2(Cl) \quad (3)$$

$$PbI_2(Cl) \xrightarrow{light} Pb + I_2 + (Cl_2) \quad (4)$$

$$PbCl_{0.6}Br_{1.4} \quad (5)$$

However, different from the decrease of PL, Chen *et al*. reported light induced PL enhancement of $MAPbX_3$ thin film at low excitations and PL quenching at high excitations in well-capsulated perovskite thin film[44]. The samples are well capsulated by PMMA and glass slip, excluding the effect of moisture and oxygen, but this report raises a question why the PL changes differently in nitrogen gas and capsulated cases, which needs further investigation.

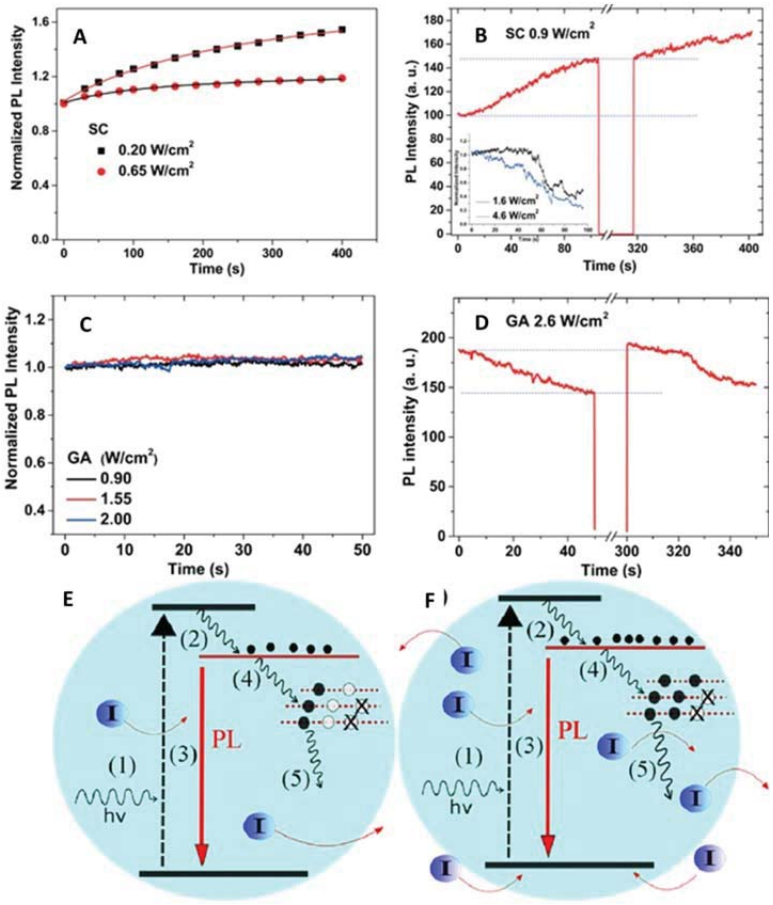

Figure 2. PL enhancement and quenching of halide perovskite thin films, reproduced with permission from Chen *et al*.[53], Copyright (2016) American Chemical Society: PL intensities of spin coating (SC) sample over time under **(A)** light excitations at 0.2 and 0.65 W/cm^2 and **(B)** light excitation at 0.9 W/cm^2, stopping at 100s for 4 minutes before resumption. PL intensities of sample fabricated by gas-assisted (GA) process over time under light excitations at **(C)** 0.90; 1.55 and 2.00 W/cm^2 and **(D)** 2.6 W/cm^2, stopping at 50s for 4 minutes before resumption. Schematics show the dynamic processes under **(E)** PL increment at low excitation; **(F)** PL quenching under high excitation. The physical processes are (1) photon excitation; (2) fast hot carrier cooling; (3) electron-hole recombination; (4) defect/surface trapping (black circle) and curing traps (cross); (5) trapped electron relaxation (detrapping) respectively.

They found the light induced effect is dependent on fabrication method. For example, the sample fabricated by convention spin coating (SC) exhibits increase in PL with light illumination, while the sample from a gas-assisted (GA) process shows a constant PL response due to a higher density of defects[44]. In detail, **Figure 2A** demonstrates that in the case of SC sample, the PL intensity increases continuously and then saturates at low excitation at 0.2 and 0.65 W/cm^2. In **Figure 2B**, the sample is firstly irradiated with laser at excitation 0.9 W/cm^2 for 100 seconds during which the PL intensity increases. Then the sample is kept in the dark for about 4 mins, and when the excitation is resumed, the PL intensity is found to remain stable. In this study, the light induced enhancement effect on the

PL of SC sample at low excitation is attributed to defect curing effect (**Figure 2E**), in which upon light illumination the defect trapping (process (4) shown by black circles in **Figure 2E**) decreases and carrier radiative recombination (process (3) in **Figure 2E**) increases, leading to increasing PL intensity in SC samples. Mosconi *et al*. reported that under illumination, Frenkel defects are annihilated[42]. In comparison, GA sample has higher density defect and the defect curing effect is trivial leading to a constant PL.

At high excitation, PL of SC samples quenches continuously and the thin film degrades, as is demonstrated in the inset of **Figure 2B**, in which the PL intensity tends to lower over time. However, PL intensity of GA sample does not change even at excitation of 2 W/cm^2 (**Figure 2C**). PL intensity of GA sample decreases with further increase of the excitation to 2.6 W/cm^2, and after being kept in dark for 4 minutes in the dark, PL intensity of GA sample changes back to its initial level (**Figure 2D**). Note that with respect to the original PL intensity, the PL at a time of 10s and at power of 4.6 W/cm^2 (46 J/cm^2) decreases, while PL at a time of 230s and at power of 0.2W/cm^2 is higher, suggesting that the excitation power is a critical parameter in determining the light induced PL changes of perovskites. The PL intensities for both samples quench under high excitations, and this results from mobile ion accumulation and increased non-radiative electron/hole recombination, as is shown in **Figure 2F**[53]. At high excitation, mobile ions can be activated probably via activation of pre-existing ions or via decomposition of the perovskite by the high density of photo-carriers. Then the ions migrate and accumulate at the grain boundary or interfaces, leading to enhanced non-radiative recombination of free carriers and consequently PL quenching[44].

2.2 In the presence of O_2 or/and moisture

As one would expect, the degradation process is more complicated when the LHPs are in the presence of oxygen. As **Table 2** demonstrates, literatures reported that in the presence of light and oxygen, for the thin films, at low excitation power and dose (power of 0.188 to 0.5 W/cm^2, dose of 33 to 150 J/cm^2), the PL enhancement is found, while decomposition is observed at higher excitation power or dose.

Table 2. The literatures of light illumination on halide perovskite in presence of O_2 or/and moisture

Material	Light illumination	Environment	Film morphology	PL	Ref
$MAPbI_3$ film	405 nm laser, 0.5 W/cm^2 for 5 mins (150 J/cm^2)	Oxygen or moisture		Continuous enhancement	[52]
$MAPbI_3$ film	532 nm, 0.188 W/cm^2 for 3 mins (33.8 J/cm^2)			Continuous enhancement	[54]
$MAPbI_3$ film	Tungsten halogen lamp (broadband), 1.5 W/cm^2 for up to 3 days (388 J/cm^2)	Oxygen	Decomposition	Not reported	[55]
$MAPbI_3$ film	<425 nm Edmund Optics, 0.1 W/cm^2 for up to 2 days (17200 J/cm^2)	Moisture	Decomposition	Not reported	[39]
$MAPbI_3$ nanocrystals	514 nm (an Argon ion laser), 10 W/cm^2 for seconds (100J/cm^2)	Air (oxygen and moisture)	Decomposition	PL intensity decreases, Blue shift	[56]

The underlying mechanism of PL enhancement is as follows: Oxygen diffuses into the films rapidly, and under light excitation of $MAPbI_3$, photoinduced electrons and holes form $MAPbI_3$*, which then transfers the electron to O_2 and produces superoxide species. Moreover, iodide vacancies are found to be the preferential sites in leading to photo-induced formation of these superoxide species from O_2[55]. This consequently removes electron trap states associated with the iodide vacancies, leading to PL enhancement of the perovskite films, as is reported by Roberto Brenes *et al*. very recently[52].

The perovskite thin film shows heterogeneous PL comprised of defect-rich dark domains and bright domains that are less defective, because of the heterogeneous distribution of trap states from grain to grain, as is shown in **Figure 3A**, **B**. Dane *et al*. conducted a detailed micro-scale study and illustrated that despite of the overall bulk PL enhancement of the films, the extent of PL enhancement varies from grain to grain. The authors found that under light illumination, dark regions with higher

trap state densities are preferentially brightened due to reduction of trap states and a redistribution in local emission intensities is also induced (**Figure 3C** shows the variation of the local emission of different spots over time)[54]. The emission of bright spot (red triangle in **Figure 3B**) only increases by a factor of 1.4, while the dark spot (blue circle in **Figure 3B**) increases by a factor of 8.7 after ~3 min of illumination. Very importantly, they also observed that reduction in the trap density is accompanied by photo-induced iodine migration: A dark spot is illuminated for several minutes with pulsed excitation (1.2 kJ cm^{-2}) and photoluminescence decay is recorded (**Figure 3D**). Iodide distribution summed through the depth in the illuminated region is shown in **Figure 3E**. The iodide distribution (columns) and laser intensity (blue curve) across the line scan (blue arrow in **Figure 3E**) in **Figure 3F** shows that the regions of highest illumination intensity have least iodide, while the adjacent regions have higher level of iodide compared to the background iodide levels, indicating migration of iodine from the illumination area to adjacent areas.

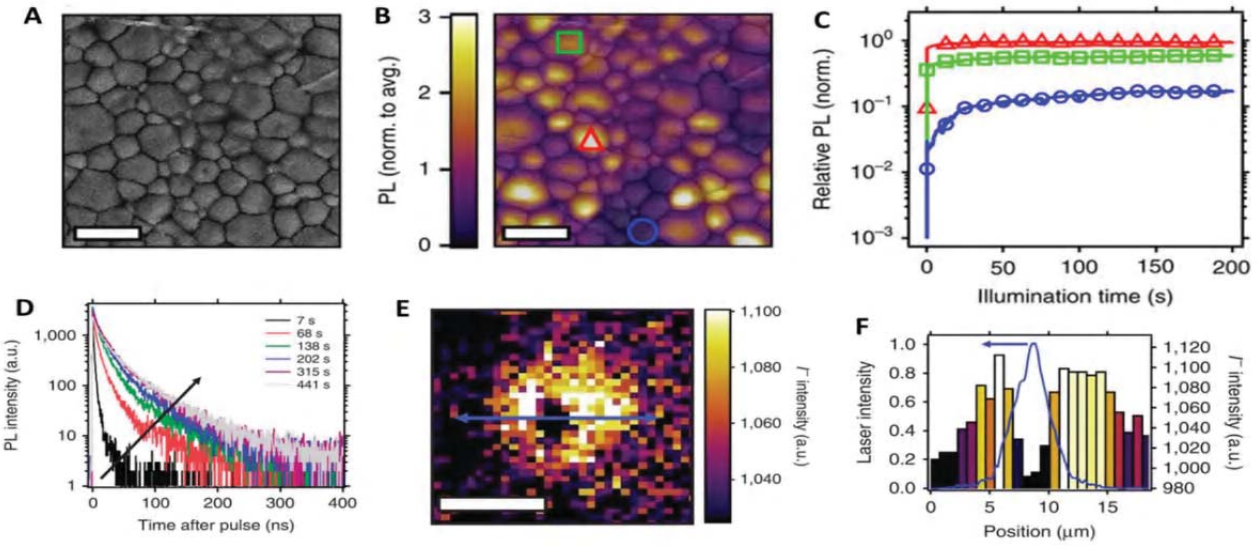

Figure 3. Microscale study of light induced PL changes of halide perovskite thin films, reproduced with permission from Dequilettes *et al*.[54], Copyright (2016) Nature Publishing Group; **(A)** Correlated scanning electron microscopy (SEM) image; and **(B)** PL image of a perovskite film measured in nitrogen with semitransparent SEM image overlaid, scale bars, 2 μm; **(C)** PL intensity over time from a dark spot (blue circles, enhancement of 8.7 times), intermediate spot (green squares, enhancement of 1.6 times) and a bright spot (red triangles, enhancement of 1.4 times) corresponding to the regions highlighted with the same symbols in **(B)**; **(D)** A series of time-resolved PL decays from a $CH_3NH_3PbI_3$ film measured over time under illumination before time-of-flight secondary-ion-mass spectrometry (ToF-SIMS) measurements; **(E)** ToF-SIMS image of the iodide (I^-) distribution summed through the film depth, scale bar, 10 μm; **(F)** Line scan of the blue arrow in **(E)** to show the iodide distribution (right axis). The measured spatial profile of the illumination laser (blue) is shown on the left axis**.**

Decomposition is also found to occur at high excitations, because the superoxide species is highly reactive and reacts with $MAPbI_3$. After reaction, $MAPbI_3$ is decomposed into methylamine, PbI_2, and I_2 through the equation (6, 7, 8) below[25,55].

$$MAPbI_3 \xrightarrow{\text{Light No moisture}} MAPbI_3^* \quad (6)$$

$$O_2 \xrightarrow{MAPbI_3^*} MAPbI_3 + O_2^- \quad (7)$$

$$\xrightarrow{\text{Deprotonation}} MeNH_2 + PbI_2 + 1/2I_2 + H_2O \quad (8)$$

The degradation in light soaking and oxygen can be reduced with several methods: production of perovskite films with large crystallites to produce less photo-induced superoxide[55], and passivation of the perovskite films with iodide salts[55].

At low excitation in the presence of moisture, under light illumination, PL is enhanced probably due to formation of a shell on the surfaces which converts the surfaces to species, which does not deteriorate the PL[52]. It is generally agreed till now that moisture alone induces hydration of $CH_3NH_3PbI_3$ films is a reversible process[31,32,57], while light illumination with high excitations in the presence of moisture induces irreversible degradation of perovskite and forms PbI_2, as is reported by Ahn *et al.*[39]. They reveal the mechanism of degradation of perovskite thin film under light illumination in the presence of moisture as follows: trapped charges are generated along the grain boundaries by light excitation, which induce local electric field, distort the structure of hydrated perovskite and trigger the ir-

reversible humidity-induced degradation of perovskite[39]. **Figure 4A** shows that in the dark condition with relative humidity (RH) 90% $MAPbI_3$ is hydrated after two days and can be dehydrated reversibly by nitrogen gas drying. However, it shows very fast irreversible degradation under light soaking even at lower RH 20% (see **Figure 4B**).

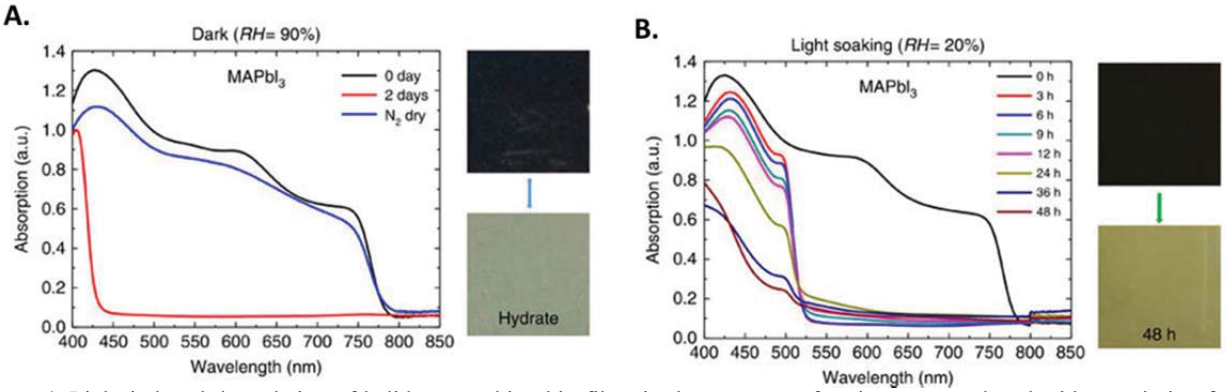

Figure 4. Light induced degradation of halide perovskite thin films in the presence of moisture, reproduced with permission from Ahn *et al.*[39], Copyright (2016) Nature Publishing Group; **(A)** Absorption spectra and pictures of the $MAPbI_3$ perovskite film and the optical images before and after ageing for two days under dark conditions at 90% RH showing that $MAPbI_3$ perovskites were transformed into transparent hydrated states after two days; **(B)** Time evolution of absorption spectra and pictures of $MAPbI_3$ before and after degradation at 20% RH under simultaneous light soaking.

In a layered geometry (thin film) the light-induced decomposition occurs at high excitations and is only on the surface, and therefore shows no spectral shift. While for the nanocrystals, the surface is high and therefore the decomposition occurs at lower excitations, and leads to clear spectra shift, shown in the last row of **Table 2**. For instance, when the solution of perovskite is spin-coated with low concentration, crystals form instead of a continuous film. Under intense light excitation, a local field gradient is induced in $MAPbI_3$ crystals, inducing migration of methylammonium ions (MA^+) which distorts the lattice structure and changes the effective band gap. The three-dimensional $MAPbI_3$ crystal structure collapses to the two-dimensional layered PbI_2 structure, as shown in **Figure 5**. The dis-tortion of the Pb–I–Pb angle caused by an increasing number of defects (ionic vacancies) lead to spectrally shifting PL[56]. It is worth noting that the effect of light illumination on PL of perovskite thin film is similar in the case of capsulated film and in the presence of oxygen or moisture. Therefore, one would need further confirmation whether the oxygen and moisture is eliminated completely in a capsulated film.

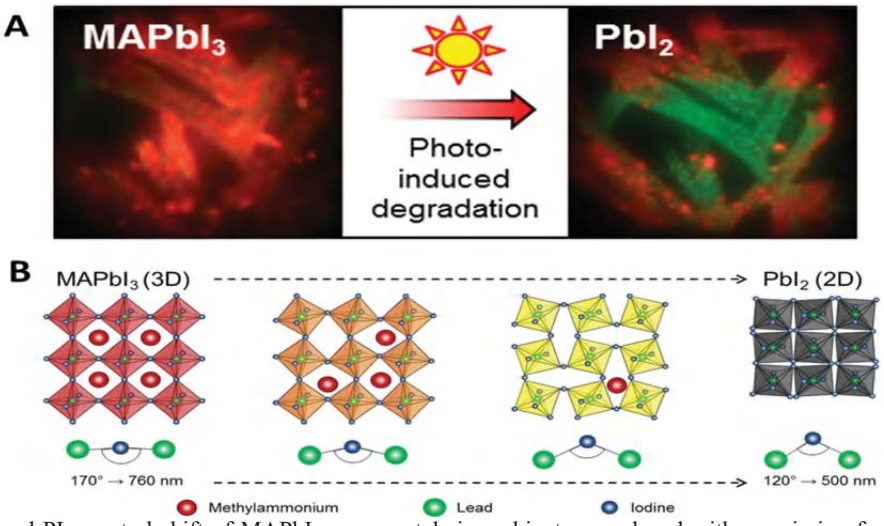

Figure 5. Light induced PL spectral shift of $MAPbI_3$ nanocrystals in ambient, reproduced with permission from ref.[56], Copyright (2016) American Chemical Society: **(A)** PL image before the degradation of a $MAPbI_3$ bulk sample and after the degradation. **(B)** Schematic showing structural change.

2.3 Light induced segregation of (MA)Pb(BrxI1-x)3 thin film

In a tandem configuration with a bottom cell with a lower bandgap (Si), perovskite material with a high bandgap of 1.7–1.8 eV is needed for the top cell. Mixed halide perovskite (MA)Pb(Br_xI_{1-x})$_3$ satisfies this requirement, however, when the excitation intensity is above a threshold, light induced reversible phase segregation occurs: upon illumination bromide and iodide ions phase segregate into Br-rich and I-rich domains with lower bandgap acting as traps and limiting the performance of solar cells[45-50].

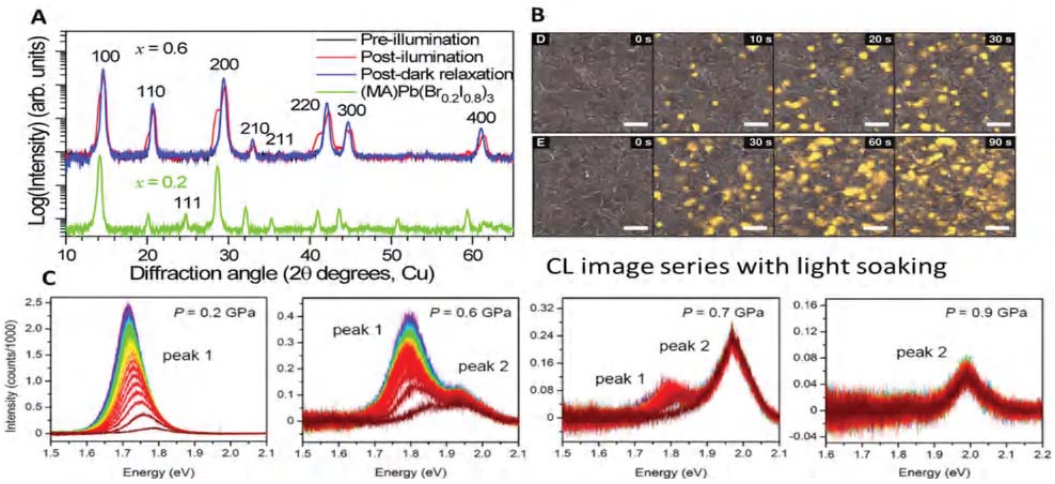

Figure 6. Light induced phase segregation in (MA)Pb(Br_xI_{1-x})$_3$ thin film: **(A)** XRD pattern of a (MA)Pb(Br_xI_{1-x})$_3$ (x = 0.6) film before (black) and after (red) white-light soaking for 5 minutes at ~50 mW cm^{-2}, and after 2 h in the dark (blue), reproduced with permission from Slotcavage *et al.*[45], Copyright (2016) American Chemical Society; **(B)** CL image series with (D) 10 and (E) 30 s of light soaking between each CL image. The scale bars are 2 μm, reproduced with permission from Bischa *et al.*[49], Copyright (2017) American Chemical Society; **(C)** PL spectra recorded Spectra displayed were obtained at 0.2 GPa, 0.6 GPa, 0.7 GPa, and 0.9 GPa, at 8 s intervals for (MA)Pb($Br_{0.6}I_{0.4}$)$_3$ showing the PL evolution with light soaking, ranging from 0 s (dark red) to 150 s (purple), reproduced with permission from Jaffe *et al.*[59], Copyright (2016) American Chemical Society.

This is evidenced by multiple experimental observations in the literatures, including XRD, PL and cathodoluminescence, and transient absorption measurements. When illuminated with white light, the original XRD pattern of (MA)Pb(Br_xI_{1-x})$_3$ thin film split into two peaks, indicating phases of two types of domains, which reverses to one peak when the sample is back to dark condition, as is shown in **Figure 6A**[45]. The ion segregation occurs through the halide defects and the I-rich domains locate at the grain boundaries in the thin film, as is demonstrated in **Figure 6B**[49]. Therefore, the segregation can be reduced by improving the crystallinity and producing larger grain sizes. The other way to minimize the segregation is through compositional tuning or compressing of the perovskite material. Bischak *et al.* suggest that by replacing MA with formamidinium (FA) or Cs the light induced segregation can be reduced, and also experimentally phase stability was reported for Cs and Cs/FA blends[49,58]. Besides, applying high pressure could also alleviate the segregation phenomenon by thermodynamically or kinetically suppress halide migration[59]. As is shown in **Figure 6C**, at a pressure of 0.9 GPa, the perovskite shows no PL red shift since light induced phase segregation is inhibited in the high-pressure phase.

3. Conclusions

In conclusion, the interaction of light and perovskite involves many physical processes depending on the environment (vacuum, nitrogen, capsulated by other layers, oxygen, moisture), light illumination conditions (excitation power, dose), and the morphology of samples (thin film or nanocrystal, the grain size of the thin film). The enhancement of PL induced by light illumination occurs at low excitations and several possible pathways reported so far can be summarized as follows: defect curing in a capsulated film; reduction of iodine vacancies associated electron traps by reaction of oxygen, photoinduced electron and hole and perovskite when

exposed to oxygen, formation of a shell by moisture to inhibit PL quenching when exposed to moisture. The quenching of PL takes place at higher light illumination, and the underlying mechanism is either by inducing defects in the case of nitrogen or vacuum, or through mobile ion accumulation and increased non-radiative electron/hole recombination in a capsulated film. At high excitations, the perovskite is also found to be decomposed into PbI_2 in the following cases: in vacuum, the volatile products desorb instantly; in an oxygen atmosphere, the reactive superoxide species are formed and decompose perovskite efficiently; in a humid environment, light generates trapped charges along the grain boundaries, which triggers the irreversible humidity-induced degradation of perovskite. Besides, in Br/I mixed halide perovskite thin film, light induces ion segregation through halide defects and the film segregates into iodine domains and bromine domains, which reverse back to the mixed halide perovskite in the dark conditions. The summary encourages us with the conclusion that the light illumination is not always detrimental for perovskite materials, and instead can be utilized to enhance the optical properties in the proper configurations and to improve the performances of perovskite-based devices. Despite the above conclusions, several points still need to be addressed such as the reason that at low excitations, PL decreases in a nitrogen atmosphere but increases in a capsulated film, in the case of PL enhancement in oxygen atmosphere at low excitations whether any morphological or compositional changes occur.

Author Contributions

Z. Y. D proposed to review, and D. A. D commented and corrected the work.

Conflict of Interest

No conflict of interest was reported by the authors.

Acknowledgement

Zhiya Dang acknowledges funding from the European Union under grant agreement No. 614897 (ERC Grant TRANS-NANO).

References

1. Pellet N, Peng G, Gregori G, *et al.* Mixed-organic-cation perovskite photovoltaics for enhanced solar-light harvesting. Angewandte Chemie International Edition 2014; 53(12): 3151–3157.
2. Eperon GE, Stranks SD, Menelaou C, *et al*. Formamidinium lead trihalide: A broadly tunable perovskite for efficient planar heterojunction solar cells. Energy & Environmental Science 2014; 7(3): 982–988.
3. Stranks SD, Snaith HJ. Metal-halide perovskites for photovoltaic and light-emitting devices. Nature Nanotechnology 2015; 10(5): 391–402.
4. Beal RE, Slotcavage DJ, Leijtens T, *et al*. Cesium lead halide perovskites with improved stability for tandem solar cells. Journal of Physical Chemistry Letters 2016; 7(5): 746–751.
5. Sjoerd A, Veldhuis, Pablo P, *et al*. Perovskite materials for light-emitting diodes and lasers. Advanced Materials 2016; 28(32): 6804–34.
6. Sum TC. Halide Perovskite Lasers. CLEO: Conference on Lasers and Electro-Optics; 2017.
7. Ahmadi M, Wu T, Hu B. A review on organic–inorganic halide perovskite photodetectors: Device engineering and fundamental physics. Advanced Materials 2017; 29(41): 1–24.
8. Wangyang P, Gong C, Rao G, *et al*. Recent advances in halide perovskite photodetectors based on different dimensional materials. Advanced Optical Materials 2018; 6(11): 1–30.
9 Dang Y, Ju D, Wang L, *et al*. Recent progress in the synthesis of hybrid halide perovskite single crystals. CrystEngComm 2016; 18(24): 4476–4484.
10. Bai S, Yuan Z, Gao F. Colloidal metal halide perovskite nanocrystals: synthesis, characterization, and applications. Journal of Materials Chemistry C 2016; 4(18): 3898–3904.
11. Yang Z, Zhang S, Li L, *et al*. Research progresses on large-area perovskite thin films and solar modules. Journal of Materiomics 2017; 3(4): 231–244.
12. Miyata A, Mitioglu A, Plochocka P, *et al*. Direct measurement of the exciton binding energy and effective masses for charge carriers in organic-inorganic tri-halide perovskites. Nature Physics 2015; 11(7): 582–587.
13. Protesescu L, Yakunin S, Bodnarchuk MI, *et al*. Nanocrystals of cesium lead halide perovskites (CsPbX3, X = Cl, Br, and I): Novel optoelectronic materials showing bright emission with wide color gamut. Nano Letters 2015; 15(6): 3692–3696.
14. Shi D, Adinolfi V, Comin R, *et al*. Low trap-state density and long carrier diffusion in organolead trihalide perovskite single crystals. Science 2015; 347 (6221): 519–522.
15. Unger EL, Kegelmann L, Suchan K, *et al*. Roadmap and roadblocks for the band gap tunability of metal halide perovskites. Journal of Materials Chemistry A 2017; 5(23): 11401–11409.
16. Liu H, Wu Z, Shao J, *et al*. $CsPb_xMn_{1-x}Cl_3$ perovskite quantum dots with high Mn substitution ratio.

ACS Nano 2017; 11(2): 2239–2247.
17. Jellicoe TC, Richter JM, Glass HFJ, *et al*. Synthesis and optical properties of lead-free cesium tin halide perovskite nanocrystals. Journal of the American Chemical Society 2016; 138(9): 2941–2944.
18. Zhang J, Yang Y, Deng H, *et al*. High quantum yield blue emission from lead free inorganic antimony halide perovskite colloidal quantum dots. ACS Nano 2017; 11(9): 9294–9302.
19. Leng M, Chen Z, Yang Y, *et al*. Lead-free, blue emitting bismuth halide perovskite quantum dots. Angewandte Chemie-International Edition 2016; 55 (48): 15012–15016.
20. Creutz SE, Siena MCD, Creutz SE, *et al*. Colloidal nanocrystals of lead-free double-perovskite (elpasolite) semiconductors: Synthesis and anion exchange to access new materials. Nano Letters; 2018; 18(2): 1118–1123.
21. Zhang L, Ju M, Liang W. The effect of moisture on the structures and properties of lead halide perovskites: A first-principles theoretical investigation. Physical Chemistry Chemical Physics 2016; 18(33): 23174–23183.
22. Ma H, Imran M, Dang Z, *et al*. Growth of metal halide perovskite, from nanocrystal to micron-scale crystal: A review. Crystals 2018; 8(5): 182.
23. Conings B, Drijkoningen J, Gauquelin N, *et al*. Intrinsic thermal instability of methylammonium lead trihalide perovskite. Advanced Energy Materials 2015; 5(15): 1–8.
24. Yang J, Siempelkamp BD, Liu D, *et al*. Investigation of $CH_3NH_3PbI_3$ degradation rates and mechanisms in controlled humidity environments using in situ techniques. ACS Nano 2015; 9(2): 1955–1963.
25. Aristidou N, Sanchez-Molina I, Chotchuangchutchaval T, *et al*. The role of oxygen in the degradation of methylammonium lead trihalide perovskite photoactive layers. Angewandte Chemie-International Edition 2015; 54(28): 8208–8212.
26. Manser JS, Saidaminov MI, Christians JA, *et al*. Making and breaking of lead halide perovskites. Accounts of Chemical Research 2016; 49(2): 330–338.
27. Dang Z, Shamsi J, Palazon F, *et al*. In situ transmission electron microscopy study of electron beam-induced transformations in colloidal cesium lead halide perovskite nanocrystals. ACS Nano 2017; 11(2): 2124–2132.
28. Dang Z, Shamsi J, Akkerman QA, *et al*. Low-temperature electron beam-induced transformations of cesium lead halide perovskite nanocrystals. ACS Omega 2017; 2(9): 5660–5665.
29. Philippe B, Park BW , Lindblad R, *et al*. Chemical and electronic structure characterization of lead halide perovskites and stability behavior under different exposures — A photoelectron spectroscopy investigation. Chemistry of Materials 2015; 27(5): 1720–1731.
30. Han Y, Meyer S, Dkhissi Y, *et al*. Degradation observations of encapsulated planar $CH_3NH_3PbI_3$ perovskite solar cells at high temperatures and humidity. Journal of Materials Chemistry A 2015; 3(15): 8139–8147.
31 Leguy AMA, Hu Y, Campoy-Quiles M, *et al*. Reversible hydration of $CH_3NH_3PbI_3$ in films, single crystals, and solar cells. Chemistry of Materials 2015; 27(9): 3397–3407.
32. Christians JA, Herrera PAM, Kamat PV. Transformation of the excited state and photovoltaic efficiency of $CH_3NH_3PbI_3$ perovskite upon controlled exposure to humidified air. Journal of the American Chemical Society 2015; 137(4): 1530–1538.
33. Brunetti B, Cavallo C, Ciccioli A, *et al*. On the thermal and thermodynamic (in)stability of methylammonium lead halide perovskites. Scientific Reports 2016; 6: 1–10.
34. Huang W, Sadhu S, Ptasinska S. Heat- and gas-induced transformation in $CH_3NH_3PbI_3$ perovskites and its effect on the efficiency of solar cells. Chemistry of Materials 2017; 29(19): 8478–8485.
35. Milosavljević AR, Huang W, Sadhu S, *et al*. Low-energy electron-induced transformations in organolead halide perovskite. Angewandte Chemie International Edition 2016; 55(34): 10083–10087.
36. Yu Y, Zhang D, Kisielowski C, *et al*. Atomic resolution imaging of halide perovskites. Nano Letters 2016; 16(12): 7530–7535.
37. Wang Y, Li X, Sreejith S, *et al*. Photon driven transformation of cesium lead halide perovskites from few-monolayer nanoplatelets to bulk phase. Advanced Materials 2016; 28(48): 10637–10643.
38. Yuan H, Debroye E, Janssen K, *et al*. Degradation of methylammonium lead iodide perovskite structures through light and electron beam driven ion migration. The Journal of Physical Chemistry Letters 2016; 7(3): 561–566.
39. Ahn N, Kwak K, Jang SM, *et al*. Trapped charge-driven degradation of perovskite solar cells. Nature Communications 2016; 7: 1–9.
40. Li Y, Xu X, Wang C, *et al*. Light-induced degradation of $CH_3NH_3PbI_3$ hybrid perovskite thin film. Joornal of Physical Chemistry C 2017; 121(7): 3904–3910.
41. Xu R, Li Y, Jin T, *et al*. In situ observation of light illumination-induced degradation in organometal mixed-halide perovskite films. Acs Applied Materials & Interfaces 2018; 10(7): 6737–6746.
42. Mosconi E, Meggiolaro D, Snaith HJ, *et al*. Light-induced annihilation of frenkel defects in organolead halide perovskites. Energy & Environmental Science 2016; 9(10): 3180–3187.
43. Li C, Zhong Y, Luna C A, *et al*. Emission enhancement and intermittency in polycrystalline organolead halide perovskite films. Molecules 2016; 21(8): 1081.
44. Chen S, Wen X, Huang S, *et al*. Light illumination induced photoluminescence enhancement and quenching in lead halide perovskite. Solar Rrl 2017; 1 (1).
45. Slotcavage DJ, Karunadasa HI, McGehee MD. Light-induced phase segregation in halide-perovskite absorbers. ACS Energy Letters 2016; 1(6): 1199–

1205.
46. Li W, Rothmann MU, Liu A, *et al*. Phase segregation enhanced ion movement in efficient inorganic $CsPbIBr_2$ solar cells. Advanced Energy Material 2017; 7(20): 1–13.
47. Yoon SJ, Draguta S, Manser JS, *et al*. Tracking iodide and bromide ion segregation in mixed halide lead perovskites during photoirradiation. ACS Energy Letters 2016; 1(1): 290–296.
48. Barker AJ, Sadhanala A, Deschler F, *et al*. Defect-assisted photoinduced halide segregation in mixed-halide perovskite thin films. ACS Energy Letters 2017; 2(6): 1416–1424.
49. Bischak CG, Hetherington CL, Wu H, *et al*. Origin of reversible photoinduced phase separation in hybrid perovskites. Nano Letters 2017; 17(2): 1028–1033.
50. Hoke ET, Slotcavage DJ, Dohner ER, *et al*. Rever sible photo-induced trap formation in mixed-halide hybrid perovskites for photovoltaics. Chemical Science 2015; 6(1): 613–617.
51. Brivio F, Caetano C, Walsh A. Thermodynamic origin of photoinstability in the $CH_3NH_3Pb(I_{1-x}Brx)_3$ hybrid halide perovskite alloy. Journal of Physical Chemistry Letters 2016; 7(6): 1083–1087.
52. Brenes R, Eames C, Bulović V, *et al*. The impact of atmosphere on the local luminescence properties of metal halide perovskite grains. Advanced Materials 2018; 30(15): 1–8.
53. Chen S, Wen X, Sheng R, *et al*. Mobile ion induced slow carrier dynamics in organic-inorganic perovskite $CH_3NH_3PbBr_3$. ACS Applied Materials & Interfaces 2016; 8(8): 5351–5357.
54. Dequilettes DW, Zhang W, Burlakov VM, *et al*. Photo-induced halide redistribution in organic-inorganic perovskite films. Nature Communications 2016; 7: 1–9.
55. Aristidou N, Eames C, Sanchez-Molina I, *et al*. Fast oxygen diffusion and iodide defects mediate oxygen-induced degradation of perovskite solar cells. Nature Communications 2017; 8: 1–10.
56. Merdasa A, Bag M, Tian Y, *et al*. Super-resolution luminescence microspectroscopy reveals the mechanism of photoinduced degradation in $CH_3NH_3PbI_3$ perovskite nanocrystals. Journal of Physical Chemistry C 2016; 120(19): 10711–10719.
57. Habisreutinger SN, Leijtens T, Eperon GE, *et al*. Carbon nanotube/polymer composites as a highly stable hole collection layer in perovskite solar cells. Nano Letters 2014; 14(10): 5561–5568.
58. McMeekin DP, Sadoughi G, Rehman W, *et al*. A mixed-cation lead mixed-halide perovskite absorber for tandem solar cells. Science 2016; 351(6269): 151–155.
59. Jaffe A, Lin Y, Beavers CM, *et al*. High-pressure single-crystal structures of 3D lead-halide hybrid perovskites and pressure effects on their electronic and optical properties. ACS Central Science 2016; 2(4): 201–209.